www.revistaft.com.br

RevistaFT | ISSN 1678-0817 | v.30, n. 159, 2026 | DOI: 10.69849/xg5xyd09

Discrete universe theory: unified effective extension from a fractal causal network *

Denivaldo Lima[1]

Abstract

We present the Discrete Universe Theory, an Effective Field Theory whose high-energy completion is described by a discrete causal network with a spectral fractal dimension of approximately 2.72, inspired by Causal Dynamical Triangulations. In this approach, continuous spacetime emerges from a fundamental discrete structure made of interconnected causal elements, while matter, fields, and observed interactions arise as collective excitations of this network.

Spectral analysis of the network Laplacian reveals a self-similar hierarchy of eigenvalues governed by the golden ratio, giving rise to a discrete tower of Kaluza-Klein modes interpreted as the internal fractal structure of quarks. The theory introduces three fundamental complex scalar fields, labeled Phi-h, Phi-l, and Phi-m, each associated with different vacuum densities and responsible for generating observable properties of matter, mass, interactions, and cosmological structure. The Phi-m field acts as a unifying component among the gravitational, dark, and cosmological sectors, while an emergent macroscopic coherence field, Psi-c, describes organized collective states of the vacuum.

The effective action preserves the gauge symmetry of the Standard Model together with an additional Abelian symmetry for a massive dark photon, enabling stable coexistence between matter and antimatter. Electromagnetism is reinterpreted as a dynamical manifestation of fundamental pairs called h-plus and h-minus, from which electric and magnetic fields, the wave-particle duality of light, and the Law of Similars naturally emerge — proposed as a microscopic principle responsible for magnetic alignment and the behavior of macroscopic magnets without violating Gauss's law.

The model further incorporates a fifth dark dimension associated with the Phi-m field, responsible for holographic movement, for interpreting quantum tunneling as transit through this energy dimension, and for the existence of non-local correlations strongly suppressed at macroscopic scales. Corpuscular light arises as a longitudinal solitonic solution of the effective electromagnetic field, while the local Planck constant becomes dynamically dependent on the vacuum density.

[1] Telecommunications Engineer, Independent Researcher
E-mail: denivlima@yahoo.com.br
* Translation note: This article is an English translation of the article originally published in Portuguese in Revista FT. The original version is available at DOI: https://doi.org/10.69849/zzqp1s46

In the cosmological sector, the theory predicts a cyclic universe with alternating phases of contraction and expansion, governed by the dynamics of the fundamental fields. A Markov Chain Monte Carlo fit using data from Planck 2018, Baryon Acoustic Oscillations, and the Pantheon-plus supernova sample yields a Hubble constant of 73.2 plus or minus 1.3 kilometers per second per megaparsec and positive Bayesian evidence (logarithm of the Bayes factor equal to plus 3.2) relative to the standard Lambda-CDM model. All currently considered experimental bounds — including those from the Large Hadron Collider, fifth-force searches, dark photon constraints, Lorentz invariance tests, and precision quantum electrodynamics — remain satisfied within the analyzed parameter space.

The theory proposes a unified framework in which spacetime, matter, fields, gravity, magnetism, and cosmology emerge from a single discrete, causal, fractal structure, providing falsifiable observational predictions and recovering, in the appropriate limits, General Relativity and the Standard Model.

Keywords: Unified field theory; unifying field; extended Einstein equations; causal network; fractal dimension; dark photon; effective field theory; quantum gravity; holographic movement; cyclic universe; law of similars; acoustic levitation; vibrational coupling.

1. Introduction

Causal Dynamical Triangulations (CDT) demonstrate that quantum spacetime can emerge from a discrete causal network with spectral fractal dimension $D_f \approx 2.72$ at the Planck scale [1,2]. This discrete structure offers a possible solution to the non-renormalizability of General Relativity (GR) and paves the way for a quantum theory of gravity. In parallel, the need to explain dark matter, dark energy, baryon asymmetry, and the recent Hubble constant tension motivates extensions of the Standard Model (SM) with new degrees of freedom, such as scalar fields and dark matter portals [3,4].

In this work, we anchor an Effective Field Theory (EFT) in the UV completion provided by CDT. The path integral over triangulated geometries is well-defined, finite, and unitary. Spectral analysis of the network Laplacian provides a self-similar Kaluza-Klein tower, whose modes we interpret as the origin of the fractal structure of quarks — a concept that echoes speculative approaches [5,6], but which here receives a rigorous mathematical formulation.

The resulting effective action extends the SM and GR with three complex scalar fields Φ_t $(t = h, l, m)$ encoding the elementary vacuum densities, an emergent macroscopic coherence field Ψ_c (analogous to an order parameter), and a massive dark photon A'_μ. The gauge symmetry $SU(3)_C \times SU(2)_L \times U(1)_Y \times U(1)_D$ is maintained, where the new $U(1)_D$ distinguishes material and dark sectors, explaining matter-antimatter coexistence without catastrophic annihilation.

The article is organized as follows. Section 2 details the UV completion and spectral analysis, deriving the KK tower and fractal structure. Section 3 presents

the complete effective action, with all sectors and interactions, and demonstrates classical stability, absence of ghosts, and optical unitarity. Section 4 lists and describes the 17 principal equations and the supporting ones, with their physical implications and recovery of classical limits. It includes the derivation of the law of similars in magnetism (Section 4.1). Section 5 describes the quantitative cosmological MCMC fit, with parameters, likelihoods, results, and Bayesian evidence, including the cyclic evolution of the universe. Section 6 confronts the model with experimental bounds (LHC, fifth-force, QED, Lorentz violation, dark photons) and presents the corrected prediction for ALPS II. Section 7 discusses the model's limitations and strategies to overcome them. Section 8 concludes the work.

2. UV Completion: Discrete Causal Network and Spectral Analysis

2.1 Path Integral on the Causal Network

The fundamental theory is defined by a sum over all four-dimensional triangulated manifolds with fixed topology and causal structure, in accordance with CDT [1,2]. The action is the Regge action [7] with matter fields allocated at the vertices:

$$S_{UV} = \sum_{simplices} \left[\frac{1}{8\pi G} (\delta - \Lambda\, a^2) V_4 + \mathcal{L}_{\text{campos}} V_4 \right], \tag{UV.1}$$

where δ is the angular deficit, $a \sim l_P$ the lattice spacing, and V_4 the four-dimensional simplex volume. The scalar fields Φ_t and fermionic fields ψ reside at the vertices, with discrete covariant derivatives defined by finite differences along the links.

The partition function is

$$Z = \sum_{T \in CDT} \frac{1}{C_T} \int \mathcal{D}\Phi e^{-S_{\text{UV}}[T,\Phi]}, \tag{UV.2}$$

where C_T is the symmetry factor of the triangulation T. The sum over geometries is finite for each fixed volume.

Unitarity: The Euclidean continuation of the path integral satisfies Osterwalder-Schrader reflection positivity [8], guaranteeing a physical Hilbert space with positive-definite inner product and unitary evolution after Wick rotation. The integration measure is positive-definite, and the quadratic action is bounded from below, eliminating ghost states.

2.2 Spectral Analysis of the CDT Laplacian

In the geometric emergence phase, the effective Laplacian □ on the network possesses a discrete spectrum with self-similarity [2]. We write the discretized operator on the Regge lattice as:

$$\Box\phi(x) = \frac{1}{\sqrt{g(x)}} \sum_{y\sim x} \frac{A_{xy}}{l_{xy}^2}[\phi(y) - \phi(x)] \ ,$$

(2.1)

where $g(x)$ is the dual volume at vertex x, A_{xy} is the area of the face dual to link xy, and l_{xy} is the link length. The causality condition restricts links to be either timelike or spacelike.

The spectral density of states $\rho(\lambda)$ for large volumes behaves as

$\rho(\lambda) \propto \lambda^{D_f/2-1}$ + periodic corrections in $\ln \lambda$. (2.2)

Discrete scale invariance, characteristic of fractals, requires that the density of states satisfy

$$\rho(\lambda) = \phi^{-D_f/2}\rho(\lambda/\phi),$$

(2.3)

for some scaling factor ϕ. The solution of (2.3) is $\phi = \frac{1+\sqrt{5}}{2} \approx 1{,}618$, the golden ratio. This follows from the functional equation $f(x) = f(\phi\, x)$, whose minimal solution is the golden ratio, which naturally appears in systems with discrete scale invariance [9].

The eigenvalues λ_n are obtained by solving the eigenvalue equation on the network:

$$\Box\phi_n = \lambda_n\phi_n.$$

(2.4)

Self-similarity imposes that the eigenvalue sequence be geometric:

$$\lambda_n = \lambda_0\phi^{2n/D_f}, \quad n = 0,1,2, \ldots$$

(2.5)

The dispersion relation on the network is $\lambda_n \propto M_n^2$; therefore, the masses of the KK modes are:

$$M_n = M_0\phi^{n/D_f},$$

(2.6)

with M_0 the fundamental scale. The normalization of the wavefunction in the fractal volume imposes

$$N_n = \phi^{n(1-2/D_f)},$$

(2.7)

such that the integral $\int dV_f\ |\psi_n|^2 = 1$.

2.3 KK Tower and Fractal Quarks

The effective fermionic field (quark) is the superposition of the KK modes:

$$q(x) = \sum_{n=0}^{\infty} \frac{1}{\sqrt{N_n}} \psi_n(x) \prod_{t=h,l,m} (1 + \lambda_{st} \mathcal{O}_t(\Phi_t)) q_0,$$

(2.8)

where $\psi_n(x)$ is the 4D field of mass M_n, $\mathcal{O}_t(\Phi_t)$ are flavor projection operators, and q_0 is the fundamental fermionic field of the SM. For energies $E \ll M_1$, only the mode $n = 0$ contributes, exactly recovering the fermions of the SM. The series is convergent and local, since the masses grow exponentially with n.

2.4 Holographic movement and the Fifth Dark Dimension

The CDT network structure reveals, beyond the four spacetime dimensions, a compactified fifth "dark" dimension, whose effective size is controlled by the field Φ_m. This extra dimension allows instantaneous transfer of information between two surfaces Σ_1 and Σ_2 separated by a distance L, without macroscopic causality violation. The entanglement entropy between the two surfaces acquires a non-local term (holographic movement), whose manifestation in the visible sector is suppressed by the coupling ϵ:

$$\boxed{S_{\text{holo}} = \epsilon^2 \frac{k_B c^3}{4G\hbar} \frac{A_1 A_2}{L^2} e^{-L/\lambda_D} \left[1 + \beta \frac{\lambda_D^2}{L^2} \ln\left(\frac{L^2}{\lambda_D^2}\right)\right].}$$

(2.9)

Here, A_1 and A_2 are the areas of the two surfaces, and $\lambda_D = \frac{\hbar c}{m_{A'}}$ is the dimensional decoupling length, controlled by the mass of the dark photon $m_{A'}$ (the first excited KK mode in the fifth dimension direction). The factor ϵ^2 reflects the coupling between the dark and visible sectors. For distances $L \gg \lambda_D$, the term is exponentially suppressed, recovering standard holography. This mechanism is the basis of action at a distance and the universal interconnection among all particles.

3. Effective Action and Stability

3.1 Effective Action of the EFT

The low-energy action, obtained by coarse-graining the network, is:

$$S_{\text{EFT}} = \int d^4x \sqrt{-g} \left[\frac{1}{2\kappa} R + \mathcal{L}_\Phi + \mathcal{L}_{\text{SM}} + \mathcal{L}_\Psi + \mathcal{L}_{\text{mistura}} + \mathcal{L}_{\text{int}}\right],$$

(A)

with $\kappa = 8\pi G/c^4$.

$\mathcal{L}_{\mathrm{SM}}$ is the complete Lagrangian of the Standard Model with gauge group $SU(3)_C \times SU(2)_L \times U(1)_Y$, three generations of fermions, Higgs boson, Yukawa couplings, and CKM and PMNS mixing matrices. Gauge anomalies cancel exactly as in the SM. The running of couplings follows the SM beta functions at low energies, receiving corrections from the new fields only above M_0.

3.1.1 Vacuum Density Field Sector Φ_t

$$\boxed{\mathcal{L}_{\Phi} = \sum_{t=h,l,m} \left[|D_\mu \Phi_t|^2 - \lambda_t(|\Phi_t|^2 - v_t^2)^2\right] - \Lambda^4_{\text{escura}}\left[1 - \cos\left(\frac{\Phi_m}{f}\right)\right]},$$

(L1)

where the covariant derivative under the group $U(1)_D$ is

$$D_\mu \Phi_t = \partial_\mu \Phi_t - i g_D Q_t^D A_\mu^D \Phi_t$$

with $Q_t^D = +1$ for material fields and $Q_t^D = -1$ for antimaterial fields. The constants $\lambda_t > 0$ guarantee potentials bounded from below. The additional cosine term for Φ_m, with scale f, introduces a long-period cyclic behavior, responsible for the systole and diastole phases of the universe [23]. The vacuum values v_t are chosen to reproduce the observed phenomenology.

3.1.2 Macroscopic Coherence Sector Ψ_c

$$\boxed{\mathcal{L}_{\Psi} = |\,\partial_\mu \Psi_c|^2 - \mu_\Psi^2 |\Psi_c|^2 - \frac{g_c}{2}|\Psi_c|^4 - \delta|\Psi_c|^2 \sum_t \gamma_t |\Phi_t|^2.}$$

(L2)

Ψ_c is an emergent complex scalar field, which parameterizes the expectation value of a composite operator of the Φ sector: $\Psi_c \sim \langle \mathcal{O}(\Phi_h, \Phi_m, \Phi_l) \rangle$. Its nature is analogous to the Ginzburg-Landau order parameter, describing the phase coherence of an underlying condensate of $h^+ h^-$ pairs. In the normal phase, $\mu_\Psi^2 > 0$ and the field is in the trivial vacuum. The transition to a coherent state ($\langle \Psi_c \rangle \neq 0$) can be induced by external sources, such as low-frequency electric fields (see Eq. 4).

3.1.3 Electromagnetic Mixing Sector (Dark Photon)

$$\boxed{\mathcal{L}_{\text{mistura}} = -\frac{1}{4}F_{\mu\nu}F^{\mu\nu} - \frac{1}{4}F'_{\mu\nu}F'^{\mu\nu} - \frac{\epsilon}{2}F_{\mu\nu}F'^{\mu\nu} + \frac{1}{2}m_{A'}^2 A'_\mu A'^\mu.}$$

(L3)

where $F_{\mu\nu} = \partial_\mu A_\nu - \partial_\nu A_\mu$ is the SM photon tensor, $F'_{\mu\nu}$ is the dark photon tensor A'_μ, ϵ is the dimensionless kinetic mixing parameter, and $m_{A'}$ is the dark photon mass generated by the Higgs mechanism in the dark sector.

3.1.4 Cross Interactions with Vibrational Coupling

The interaction Lagrangian is extended to include a coupling between the mechanical strain tensor $\sigma^{\mu\nu}$ of the material medium and the mass fields Φ_m, $\Phi_{\bar{m}}$. This term is motivated by the observation that coherent vibrations (acoustic) can alter the effective density of $m^{\pm}$ pairs, locally modulating mass.

$$\mathcal{L}_{\text{int}} = \sum_{t \neq t'} \frac{g_{tt'}}{\Lambda^2} |\Phi_t|^2 |\Phi_{t'}|^2 + \sum_t \lambda'_t |\Phi_t|^4 + \delta |\Psi_c|^2 \sum_t \gamma_t |\Phi_t|^2 + \mathcal{L}^{\text{novo}}_{\text{Yukawa}}$$

$$+ \frac{\xi_{ress}}{\Lambda^2_{ress}} \sigma^{\mu\nu} (\partial_\mu \Phi_m \, \partial_\nu \Phi_{\bar{m}} + \partial_\mu \Phi_{\bar{m}} \, \partial_\nu \Phi_m). \quad \text{(L4)}$$

Description of the new parameters:

- $\sigma^{\mu\nu}$: mechanical stress tensor of the material, which describes acoustic stresses and vibrations. In a solid, $\sigma^{\mu\nu}$ contains the phonon modes and can be expressed in terms of the displacement field $\boldsymbol{u}$.

- Λ_{ress}: characteristic energy scale of the resonant coupling. For ordinary materials, it is expected to be in the meV to eV range, corresponding to acoustic frequencies from kHz to MHz.

- ξ_{ress}: dimensionless coupling constant of order $\mathcal{O}(1)$.

This term respects the $U(1)_D$ symmetry (both fields have opposite charges, making the product $D_\mu \, \Phi_m \, D_\nu \, \Phi_{\bar{m}}$ invariant). Under normal conditions, $\sigma^{\mu\nu}$ is negligible or random, and the new term does not contribute. Under intense coherent vibrations, it acts as an external source for the relative dynamics between Φ_m and $\Phi_{\bar{m}}$, enabling effective mass modulation via Eq. (5).

3.2 Kinetic Diagonalization and Absence of Ghosts

Expanding each scalar field around its VEV, $\Phi_t = (v_t + \phi_t) e^{i\theta_t}$, the kinetic terms become:

$$\mathcal{L}_{\text{kin}} = \sum_t [(\partial \phi_t)^2 + v_t^2 (\partial \theta_t)^2] + (\partial \Psi_c)^2. \quad \text{(3.1)}$$

All fields have positive kinetic sign (+), implying that the propagators have no poles with negative residue. For the gauge sector, the kinetic mixing matrix between A_μ and A'_μ is diagonalized by a rotation of angle $\epsilon/2$, resulting in a massless photon and a massive dark photon, both with well-behaved propagators.

3.3 Optical Unitarity

The unitarity of the S -matrix is verified by requiring that scattering amplitudes satisfy the optical theorem order by order in the perturbative expansion. For the

new sectors, the decay widths are much smaller than the masses ($\Gamma \ll M$), preserving perturbative unitarity. The absence of tachyons ($m^2 > 0$ for all fields) is guaranteed by the choice of VEVs and positive coupling constants.

3.4 Potential Stability

The complete scalar potential is:

$$V = \sum_t \lambda_t(|\Phi_t|^2 - v_t^2)^2 + \Lambda_{\text{escura}}^4\left[1 - \cos\left(\frac{\Phi_m}{f}\right)\right] + \mu_\Psi^2|\Psi_c|^2 + \frac{g_c}{2}|\Psi_c|^4 + \delta|\Psi_c|^2\sum_t \gamma_t|\Phi_t|^2 + \sum_{t\neq t'}\frac{g_{tt'}}{\Lambda^2}|\Phi_t|^2|\Phi_{t'}|^2. \quad (3.2)$$

The boundedness-from-below condition requires the quartic coupling matrix to be copositive. Sufficient conditions are:

$$\lambda_t > 0, g_c > 0, \delta\gamma_t > -2\sqrt{\frac{\lambda_t g_c}{2}}, g_{tt'} > -2\sqrt{\lambda_t\lambda_{t'}}. \quad (3.3)$$

For natural values $\lambda_t \sim \mathcal{O}(1)$, $g_c \sim \mathcal{O}(1)$, $|\delta| \ll 1$ and $|g_{tt'}| \ll 1$, the potential is stable. Radiative stability analysis via the renormalization group (RG flow) confirms that the conditions hold up to the cutoff scale Λ. The Hamiltonian is positive-definite.

4. The 17 Equations of Motion and Supporting Ones

Equation 1 – Unifying Field (Modified Einstein)

The Unifying Field Equation emerges naturally from the coarse-graining process of the discrete causal network described by Causal Dynamical Triangulations (CDT), where the path integral over triangulated geometries at the Planck scale produces, in the low-energy limit, an effective action that extends GR with new fields and interactions.

$$\boxed{\frac{1}{\kappa}G_{\mu\nu} + T_{\mu\nu}^{(\text{SM})} + T_{\mu\nu}^{(\Phi)} + T_{\mu\nu}^{(\Psi)} + T_{\mu\nu}^{(\text{mistura})} + T_{\mu\nu}^{(\text{int})} = 0.} \quad (1)$$

GR Recovery: In the vacuum $\Phi_t \to v_t$ and $\Psi_c \to 0$, the extra tensors reduce to an effective cosmological constant $\Lambda_{eff}\, g_{\mu\nu}$, recovering standard GR with a cosmological constant.

Equation 2 – Fractal Quarks (Discrete KK Tower)

Here we present a reinterpretation of the nature of quarks in light of the Discrete Universe Theory. Our central thesis is that quarks are not elementary particles in the usual sense, but rather low-energy manifestations of a much richer structure: an infinite tower of Kaluza-Klein (KK) modes that emerges naturally from the fractal geometry of the discrete causal network at the Planck scale. The central equation encapsulating this idea is:

$$q(x) = \sum_{n=0}^{\infty} \frac{1}{\sqrt{N_n}} \psi_n(x) \prod_t (1 + \lambda_{st} \mathcal{O}_t(\Phi_t)) q_0. \tag{2}$$

with $M_n = M_0\, \phi^{n/D_f}$, $N_n = \phi^{n(1-2/D_f)}$, $D_f \approx 2.72$, $\phi = (1+\sqrt{5})/2$, and $M_0 > 10\ TeV$. The mode $n = 0$ recovers the SM quarks.

Equation 3 – Strong Force with Scalar Correction

Although extremely successful, the Cornell potential is a phenomenological description derived from fits to experimental data. QCD, in its fundamental formulation, predicts this behavior through non-perturbative calculations (such as lattice QCD), but a complete analytical derivation remains a challenge. Moreover, standard QCD does not consider the possibility that the parameters α_s and σ may vary in extreme environments, such as inside neutron stars, in the primordial universe, or in regions where the vacuum density fields differ from their galactic vacuum values.

Thus, Equation 3 extends the Cornell potential to include a correction dependent on the gravitational vacuum density field Φ_m:

$$V(r) = \left(-\frac{4}{3}\frac{\alpha_s(r)}{r} + \sigma r\right)\left[1 + \epsilon\left(\frac{|\Phi_m|^2 - v_m^2}{v_m^2}\right)e^{-r/\lambda_f}\right]. \tag{3}$$

$\sigma \approx 0{,}18\ GeV^2, \epsilon \ll 1,\ \lambda_f \sim 1\ fm$. In the vacuum, the standard Cornell potential of QCD is recovered.

Equation 4 – Macroscopic Quantum Coherence

The present theory postulates the existence of a complex scalar field Ψ_c that plays a role analogous to an order parameter, but in a much more fundamental context. Ψ_c does not describe a condensate of atoms or Cooper pairs, but rather the phase coherence of an underlying condensate of $h^+\, h^-$ pairs — the elementary excitations of the discrete causal network that, at low energies,

manifest as the constituents of the electromagnetic field and the vacuum density fields.

The central equation governing the dynamics of Ψ_c is:

$$\boxed{i\hbar\,\partial_t\Psi_c = \left[-\frac{\hbar^2}{2m_{\backslash\text{eff}}}\nabla^2 + g_c|\Psi_c|^2 - \delta\sum_t \gamma_t|\Phi_t|^2 + \eta\boldsymbol{E}_{\text{deg}}\cdot\boldsymbol{p}\right]\Psi_c.} \quad (4)$$

where $\boldsymbol{E}_{deg}$ is the low-frequency component of the applied electric field, $\boldsymbol{p}$ is the dipole moment, and $\eta \approx ea_0/\hbar$. Vortex solutions ("ball lightning") emerge for $g_c > 0$ and an appropriate external field.

Equation 5 – Physical Mass with Reinterpreted Sign

Modern cosmology reveals that the universe contains far more matter than antimatter. The baryon asymmetry,

$$\eta_B = \frac{n_B - n_{\bar{B}}}{n_\gamma} \approx 6\times 10^{-10},$$

indicates that for every billion particle-antiparticle pairs annihilated in the primordial universe, approximately one matter particle survived. The Sakharov conditions — baryon number violation, C and CP violation, and thermal disequilibrium — are satisfied in the SM, but the magnitude of the generated asymmetry is insufficient by several orders of magnitude.

Here we address both issues — the origin of mass and matter-antimatter asymmetry — through a unified mechanism centered on the vacuum density fields — in particular, the field associated with gravitational mass, ϕ_m, and its antimatter conjugate, $\phi_{\bar{m}}$, whose densities determine the dynamic contribution of the vacuum to the effective mass, while the other vacuum fields contribute through extended Yukawa couplings. The central equation is:

$$\boxed{m_{eff} = y\phi_H + \kappa_m\hbar\omega_v(|\Phi_m|^2 - |\Phi_{\bar{m}}|^2),\ m_{phys} = |m_{eff}|.} \quad (5)$$

$y\phi_H$ is the Higgs Yukawa coupling. For SM particles, the Higgs term dominates, ensuring $m_{phys} > 0$. The negative sign in the dark sector only indicates a shifted vacuum; the rest energy is always positive. CPT symmetry is preserved in the symmetric vacuum ($|\Phi_m| = |\Phi_{\bar{m}}|$), where particle and antiparticle masses are identical. The scale $\hbar\,\omega_v$ is not the oscillation frequency of Φ_m, but a free parameter of the EFT inherited from the CDT network, which can be fixed by observations (e.g., $\hbar\,\omega_v \lesssim 10^5\ eV$ so as not to exceed the electron mass).

The Klein-Gordon equations for Φ_m and $\Phi\_\bar{m}$ include the vibrational source term:

$$\square\,\Phi_m + \lambda_m\,(|\Phi_m|^2 - v_m^2)\Phi_m + \frac{g_{hm}}{\Lambda^2}\,|\Phi_h|^2\,\Phi_m + \cdots = \frac{\xi_{ress}}{\Lambda_{ress}^2}\,\nabla_\mu\,(\sigma^{\mu\nu}\,\partial_\nu\Phi_{\bar{m}}).$$

(5a)

$$\square\,\Phi_{\bar{m}} + \lambda_m\,(|\Phi_{\bar{m}}|^2 - v_{\bar{m}}^2)\Phi_{\bar{m}} + \frac{g_{hm}}{\Lambda^2}\,|\Phi_h|^2\,\Phi_{\bar{m}} + \cdots = \frac{\xi_{ress}}{\Lambda_{ress}^2}\,\nabla_\mu(\sigma^{\mu\nu}\,\partial_\nu\,\Phi_m).$$

(5b)

These equations show that coherent vibration (oscillating (σ^$\mu\nu$ can transfer energy to the antimaterial field $\Phi_{\bar{m}}$, reducing the net density $|\Phi_m|^2 - |\Phi_{\bar{m}}|^2$ and, consequently, the effective mass.

Equation 6 – Vacuum Saturation (Cyclic Evolution)

In a different perspective on the history and destiny of the cosmos, instead of a singular Big Bang followed by eternal expansion, we have a cyclic universe, with alternating phases of expansion (diastole) and contraction (systole), driven by the dynamics of the vacuum density field Φ_m and its antimatter partner $\Phi_{\bar{m}}$. The equation governing this cycle is:

$$\boxed{\sum_t (\langle|\Phi_t|^2\rangle - \langle\,|\Phi_{\bar{t}}|^2\,\rangle) = C_{vácuo}(t),}$$

(6)

where $C_{vácuo}(t)$ is a slowly varying function in cosmological time, reflecting the systole and diastole phases of the universe. At the present stage, $C_{vácuo}$ is adjusted to reproduce the observed dark energy density ($\rho_\Lambda \sim 10^{-47}\,GeV^4$) in Planck units).

Equation 7 – Quantum Holography with Holographic movement

The holographic paradigm is extended to incorporate a fifth dark dimension, whose dynamics is controlled by the vacuum density field Φ_m. This extra dimension is not an ordinary spacetime, but an "internal" dimension that emerges from the fractal structure of the discrete causal network. It allows non-local transfer of information between two surfaces separated by a distance L, without macroscopic causality violation. This phenomenon is called holographic movement.

The central equation quantifies the entanglement entropy between two surfaces mediated by holographic movement and explicitly incorporates the coupling factor to the visible sector and the appropriate length scales:

$$\boxed{S_{\text{holo}} = \epsilon^2\,\frac{k_B c^3}{4G\hbar}\,\frac{A_1 A_2}{L^2}\,e^{-L/\lambda_D}\left[1 + \beta\,\frac{\lambda_D^2}{L^2}\ln\left(\frac{L^2}{\lambda_D^2}\right)\right].}$$

(7)

For $L \ll \lambda_D$, the maximum holographic movement term is recovered; for $L \gg \lambda_D$, the entropy is exponentially suppressed, preserving macroscopic causality. The scale $\lambda_D = \hbar / mA'c$ is the decoupling length of the fifth dimension, and the factor $\epsilon^2 \sim 10^{-24}$ suppresses the entropy accessible to the visible sector.

Equation 8 – Electromagnetism as Dynamics of $h^{\pm}$ Pairs and Corpuscular Light

Despite the success of electromagnetism, fundamental questions remain open: what is the ultimate nature of the electromagnetic field? What are photons really? How does wave-particle duality emerge from more fundamental principles? In modern physics, the photon is described as a massless elementary particle, the quantum of the electromagnetic field. Its wave-particle duality is a postulate of quantum mechanics, not a consequence derived from an underlying structure.

But electromagnetism arises from the quantum dynamics of $\boldsymbol{h}^{+}\,\boldsymbol{h}^{-}$ pairs — the elementary excitations responsible for the magnetic field of the discrete causal network. In this framework, the electromagnetic potential $P_\mu \, or \, A_\mu$ is not a fundamental field, but an effective description of the density and collective orientation of dipoles formed by these pairs. The central equation governing this dynamics is:

$$\boxed{\Box \mathcal{P}_\mu = \mu_0 \left[\rho_+ J_\mu^{(+)} + \rho_- J_\mu^{(-)}\right] + \lambda(\rho_+ - \rho_-)\, \partial_\mu(\partial_\nu \mathcal{P}^\nu).}$$

(8a)

with $\rho_\pm = |\Phi_h|^2$, $|\Phi_\hbar|^2$, and $F_{\mu\nu} = \partial_\mu P_\nu - \partial_\nu P_\mu$. In the symmetric vacuum ($\rho_+ = \rho_-$), the equation reduces to $\Box P_\mu = \mu_0 J_\mu$, exactly recovering Maxwell's equations in the Lorenz gauge.

Corpuscular mode (longitudinal soliton): In asymmetric vacuum ($\rho_+ \neq \rho_-$), the equation admits localized soliton solutions:

$$\boxed{\Psi_{\text{fóton}}(x,t) = \Psi_0 \operatorname{sech}\left(\frac{x - vt}{\Delta}\right) e^{i(kx - \omega t)}, \Delta = \frac{\hbar}{\sqrt{2 m_{\text{eff}} g_c |\Psi_0|^2}}.}$$

(8b)

The corpuscle energy is $E = n\, h_{eff} \nu$), concentrated in the upper half-wave [5,6]. Wave-particle duality emerges naturally as the transition between the transverse mode (symmetric vacuum) and the longitudinal soliton mode (asymmetric vacuum).

Gauge analysis: The tensor $F_{\mu\nu}$ is invariant under $P_\mu \to P_\mu + \partial_\mu \Lambda$. In the asymmetric vacuum, the equation corresponds to that of a massive photon (Proca), whose gauge invariance is restored by the Stückelberg mechanism. The mass $m_{eff}^2 = \lambda\,(\rho_+ - \rho_-)$ is medium-induced, without fundamental breaking of

the $U(1)_{EM}$ symmetry. Ward identities are satisfied and the propagator has no ghost poles.

Equation 9 – Tunneling as Transit through the Fifth Dark Dimension

The standard WKB formula is derived in the context of a four-dimensional spacetime without additional internal structure. If spacetime possesses extra dimensions, such as the aforementioned fifth dark dimension, the tunneling process can be profoundly modified. The particle is no longer confined to crossing the barrier only in 4D; it can "detour" through the extra dimension, finding a shorter path or a reduced effective barrier. In terms of the fundamental hologram, tunneling is a journey through energy, transiting between the different density levels of the material and dark vacuum. Equation 9 generalizes the WKB formula to include this effect, replacing the potential V with an effective potential V_{eff} that depends on the relative density of the mass fields:

$$\Gamma = exp\left[-\frac{2}{\hbar} \int_{r_1}^{r_2} \sqrt{2m\,[\,V(r) - E\,]\left(1 - \kappa \frac{|\Phi_{\bar{m}}|^2}{|\Phi_m|^2 + |\Phi_{\bar{m}}|^2}\right)}\; dr \right] \tag{9}$$

Description of terms:

- Γ: tunneling probability (dimensionless).

- The term $2m[V(r) - E]$ is the standard WKB term, representing the squared momentum of the particle under the barrier in the visible sector.

- $|\Phi_m|^2$ and $|\Phi_{\bar{m}}|^2$: densities of the material and dark mass fields, respectively. The ratio $\frac{|\Phi_{\bar{m}}|^2}{(|\Phi_m|^2 + |\Phi_{\bar{m}}|^2)}$ measures the participation of the dark sector in the local vacuum density.

- κ: dimensionless coupling constant of order $\mathcal{O}(1)$, parameterizing the efficiency with which the particle can access the dark plane to bypass the barrier.

Physical interpretation and dimensional consistency:

- **Dimensionality**: The term in brackets is dimensionless $(1 - \kappa \times \text{dimensionless ratio})$. Therefore, the dimension of the radicand remains $2m(V - E)$, which is [momentum]². The square root gives [momentum], and the integral $\int (momentum)\, dr$ has the dimension of action. Divided by $\hbar$, the exponential is dimensionless. The equation is dimensionally correct.

- **Recovery of standard WKB**: In the visible sector vacuum, where the dark matter density is tiny ($|\Phi_{\bar{m}}|^2 \ll |\Phi_m|^2$), the ratio tends to zero, and $V_{eff}(r) \approx V(r)$. The formula reduces exactly to the standard WKB, recovering all established results for tunneling in nuclear and solid-state physics.

- **Tunneling amplification by the dark sector**: In regions where the dark energy density is significant ($|\Phi_{\bar{m}}|^2 \sim |\Phi_m|^2$), the factor $\left(1 - \kappa \frac{|\Phi_{\bar{m}}|^2}{|\Phi_m|^2+|\Phi_{\bar{m}}|^2}\right)$ reduces the effective barrier. For $\kappa \sim 1$, the barrier can be reduced by up to half, resulting in an exponential increase in the tunneling probability. This is the mechanism by which transit through the energy dimension (the "holographic shortcut") amplifies quantum processes forbidden under normal conditions.

- **Scale hierarchy**: The effect depends purely on vacuum densities, not on length scales such as λ_D or l_P, eliminating previous hierarchy problems. The energy scale relevant to tunneling remains that of the particle and the barrier, but the presence of the dark plane distorts the barrier in a dimensionless manner.

Illustrative example: For an alpha particle in a region with $\frac{|\Phi_{\bar{m}}|^2}{|\Phi_m|^2} \sim 10^{-6}$ (galactic dark matter density), the correction is one part in a million, negligible. In contrast, inside a neutron star or near a black hole, where densities can become comparable, tunneling can be drastically amplified, affecting nuclear reaction rates and stellar evolution.

Equation 10 – Electogravity (Covariant Extended Maxwell)

The interaction between gravitation and electromagnetism has been a recurring theme in theoretical physics since the 19th century. Unification attempts, from Kaluza-Klein theories to General Relativity with gauge fields, generally introduce extra dimensions or geometric modifications. Here, what is proposed is a direct coupling, albeit extremely tenuous, between the gravitational mass density and the electromagnetic field, mediated by the vacuum density fields Φ_m and $\Phi_{\bar{m}}$. This coupling gives rise to electrogravity — a modification of Maxwell's equations that includes, in addition to the usual electric current, a mass current and a macroscopic quantum coherence current. The equation is:

$$\boxed{\nabla_\nu F^{\mu\nu} = \mu_0\left(J^\mu_{\text{el}} + \xi_g J^\mu_{\text{massa}} + \zeta_c J^\mu_{\text{coer}}\right),\ \nabla_\nu \tilde{F}^{\mu\nu} = 0.} \tag{10}$$

$J^\mu_{massa} = \rho_0(|\Phi_m|^2 - |\Phi_{\bar{m}}|^2)u^\mu$, $\xi_g \lesssim 10^{-30}$, $\zeta_c \approx e$,
$J^\mu_{\text{coer}} = i\hbar(\Psi_c^* \partial^\mu \Psi_c - \Psi_c \partial^\mu \Psi_c^*)$. In the local vacuum, it recovers Maxwell's equations exactly. The extremely small value of ξ_g does not render the term irrelevant: it can generate measurable electric fields in compact objects such as neutron stars, where the mass density is $10^{14}\ g/cm^3$.

Equation 11 – Fundamental Forces, Magnetic Interaction, and the Law of Similars

Nature exhibits four fundamental interactions: the strong force, the electromagnetic force, the weak force, and gravity. In the low-energy limit, these forces manifest as interaction potentials between particles. Here, we postulate

that all these potentials emerge naturally as different manifestations of a single underlying interaction among the excitations of the discrete causal network. Moreover, it explains, from first principles, the enigmatic behavior of macroscopic magnets: why opposite poles attract, why a broken magnetic bar generates new poles, and why it is impossible to isolate a magnetic monopole. The central equation is Equation 11, which expresses the interaction potential between two particles i and j as:

$$V_{ij} = \frac{1}{4\pi}\left[\frac{q_i q_j}{r} + \frac{q_D^i\, q_D^j}{r} e^{-m_D r}\right] - \kappa_{align}(t_i, t_j)\frac{\mu_0}{4\pi r^3}\left[\,3(\vec{\mu}_i \cdot \hat{r})(\vec{\mu}_j \cdot \hat{r}) - \vec{\mu}_i \cdot \vec{\mu}_j\right], \tag{11}$$

$\kappa_{align} = +1$ for particles of the same type $(t_i = t_j)$, recovering the standard dipole interaction and ferromagnetism; $\kappa_{align} = -1$ for opposite types, relevant only in the dark sector. For the electromagnetic sector $(q_D = 0)$, Coulomb's law is exact.

Equation 12 – Modified Gravity (Newtonian Limit)

Observations in recent decades — such as flat rotation curves of spiral galaxies, the dynamics of galaxy clusters, and the accelerated expansion of the universe — have revealed discrepancies requiring the introduction of dark matter and dark energy. These exotic components, although phenomenologically successful, lack a definitive microscopic foundation. The proposal is that low-energy gravitation is modified by the presence of the vacuum density fields Φ_m, $\Phi_{\bar{m}}$ and Φ_l. These modifications manifest as additional sources in the Poisson equation, transforming it into Equation 12:

$$\nabla^2 \Phi_{grav} = 4\pi G \rho_0 \left(|\Phi_m|^2 - |\Phi_{\bar{m}}|^2 \right) + \lambda_m \nabla \cdot J_m + \lambda_l \nabla \cdot J_l + \Lambda_{eff}\, c^2, \tag{12}$$

with $\lambda_t = l_P^2/\hbar$. The current terms are suppressed by the Planck scale and consistent with fifth-force tests.

Equation 13 – Gravitational Buoyancy (Archimedes Generalized to the Quantum Vacuum)

Archimedes' principle, formulated in the 3rd century BC, is one of the cornerstones of hydrostatics: "A body immersed in a fluid experiences an upward force equal to the weight of the displaced fluid." This force, known as buoyancy, is why ships float, balloons rise in the atmosphere, and convection currents form in the Earth's mantle. Buoyancy is a direct consequence of the pressure gradient in the fluid, which in turn is related to the gravitational field.

Here, this principle is extended to the quantum vacuum, treating the vacuum density fields Φ_m and $\Phi_{\bar{m}}$ as a continuous medium that permeates all space. In

this view, any material object is not only immersed in spacetime, but also in a "vacuum fluid" whose effective density is determined by $|\Phi_m|^2$. Consequently, the net buoyancy force on a region V is the difference between the gravitational force on the material content of the region and the force that would act on the same volume filled only with the background vacuum. Equation 13 formalizes this principle of Archimedes generalized to the quantum vacuum:

$$F_{emp} = -\int_V \rho_0 \, (|\Phi_m|^2 - v_m^2) \nabla \Phi_{grav} \, dV + \left(\kappa_0 \int_V |\Psi_c|^2 dV \right) \nabla \langle \, \Phi_{\bar{m}} \, \rangle^2 \times B_{grav} \tag{13}$$

Interpretation of terms:

- **First term (quantum Archimedes buoyancy)**: The integral contains the difference between the material vacuum density inside the region $(|\Phi_m|^2)$ and the background value (v_m^2). When $|\Phi_m|^2 < v_m^2$ — a situation achieved by injecting the antimaterial field $\Phi_{\bar{m}}$ into the region — the effective density becomes smaller than that of the ambient vacuum, generating a force opposite to the gravitational gradient (upward, levitation). This mechanism corresponds exactly to that described in the text: "in the levitation of matter we gather $\bar{m}$ particles below the bodies, and m particles above, thus canceling the gravitational effect."

- **Second term (coherence)**: The contribution of the macroscopic coherence field Ψ_c, with coupling $\kappa_0 \sim 10^{-15}$. For non-coherent matter, this term is null, but in states of $h^+ \, h^-$ pair condensates, it can provide an additional force of the gravitational Magnus type.

Recovery of established physics: Under normal conditions, $|\Phi_m|^2 \approx v_m^2$ and $\Psi_c \approx 0$, canceling both terms and recovering standard Archimedes physics (no buoyancy at rest). Levitation only manifests when the material vacuum density is actively reduced below the background value — an exceptional condition requiring engineering of elementary fields or vibrational resonance (Eq. 5a-5b).

Equation 14 – Causal Network (Regge Action)

The search for a quantum theory of gravity has led physicists to explore the possibility that spacetime, at the Planck scale, is not a smooth continuum, but rather a discrete structure. A discretization of the Einstein-Hilbert action of General Relativity was proposed by Tullio Regge in 1961, who proposed replacing continuous curvature with angular deficits concentrated on codimension-2 submanifolds (the hinges), and the volume integral with a sum over the volumes of simplices. Equation 14 expresses this fundamental action governing the dynamics of the causal network at the Planck scale:

$$S_{\text{rede}} = \sum_{\text{simplices}} \left[\frac{1}{8\pi G} (\delta - \Lambda a^2) V_4 + \text{boundary terms} \right].$$

(14)

Equation 15 – Lorentz Invariance and Local Planck Constant

The systematic idea of the theory takes into account that the coupling constants and masses depend on the values of the vacuum density fields, which are dynamic. In particular, the Planck constant h — the scale of quantum action — must depend on the field Φ_h, which is associated with the electric charge density of the vacuum, because the electric charge is linked to the structure of $h^+ h^-$ pairs (Equation 8), and the field Φ_h controls the density of these pairs. The quantization of action, encapsulated in h, emerges from the collective dynamics of these pairs. If the pair density changes, the scale of quantum action also changes. Thus, the Planck constant may not be absolute, but depend on the local density of the vacuum field Φ_h, the field associated with electric charge and the electromagnetic vacuum energy density. This dependence can be expressed by Equation 15:

$$\boxed{p_\mu p^\mu = m^2c^4,\ p_\mu = h_{\text{eff}}(\Phi_h)k_\mu,\ h_{\text{eff}}(\Phi_h) = h_0\frac{|\Phi_h|^2}{v_h^2}.}$$

(15)

The dispersion relation is covariant; the variation of h_{eff} with local density does not break Lorentz invariance, as it merely redefines the local energy scale. The quadratic dependence on $|\Phi_h|$ is fixed by scale invariance: the photon kinetic term $F_{\mu\nu}\,F^{\mu\nu}$ requires $F_{\mu\nu}$ to scale with the field density, and the simplest relation compatible with the symmetries is $h_{eff} \propto |\Phi_h|^2$.

Equation 16 – Modified Cosmological Redshift with Cubic Dependence

In the standard interpretation of General Relativity, the cosmological redshift (z) of a distant galaxy is caused by the expansion of spacetime: the wavelength of the emitted light is stretched proportionally to the scale factor of the universe between the time of emission and the time of observation.

It so happens that the atomic transition energies, which determine the frequencies of light emitted and absorbed by atoms, vary with h_{eff}^{-3} — the famous cubic dependence. If the value of $|\Phi_h|^2$ at the time and place of emission was different from the current value in the Solar System, the observed redshift (z_{obs}) is not simply (z_{cosmo}), but incorporates an additional correction. Equation 16 proposes this correction:

$$\boxed{z_{\text{obs}} = (1 + z_{\text{cosmo}})\left[1 + \alpha_z\int\frac{\partial_t\Phi_m}{c}dl + \beta_z\int\frac{\partial_t|\Phi_h|^2}{c}dl\right]\left(\frac{|\Phi_h|^2_{\text{emit}}}{|\Phi_h|^2_{\text{obs}}}\right)^{-3} - 1\}.}$$

(16)

$\alpha_z, \beta_z \sim 10^{-5}$. The factor $\left(\frac{|\Phi_h|^2_{\text{emit}}}{|\Phi_h|^2_{\text{obs}}}\right)^{-3}$ captures the cubic dependence of the atomic transition frequency on the local Planck constant (Rydberg constant $\propto h_{eff}^{-3}$), as described in Appendix A of [5]. The electric charge e is considered constant because it is associated with the fundamental charge of the $h^+ h^-$ pairs. The term z_{cosmo} is the standard redshift of metric expansion.

Equation 17 – Existence Index with Holographic movement

Decoherence theory explains that quantum systems inevitably interact with their environments, and this interaction rapidly destroys the phase coherence among the different states of the superposition. Here we expand this paradigm by introducing a new decoherence channel — and therefore a new time scale — mediated by holographic movement (Equation 7) and the vacuum density fields. The expansion is expressed in Equation 17, which defines an Existence Index to quantify the degree of "classicality" of an object:

$$t_{\text{deco}} = \frac{\hbar}{k_B T_{\text{eff}} \left(1 + \gamma \sum_t |\Phi_t|^2 + \zeta \frac{A}{L^2} e^{\frac{-L}{\lambda_D}}\right)}, \mathcal{E} = \frac{t_{\text{deco}}}{t_P}. \quad (17)$$

Operational criterion: $\mathcal{E} \gg 1$ implies a classical object; $\mathcal{E} \ll 1$ indicates an object indistinguishable from the vacuum. The term $\zeta \frac{A}{L^2} e^{-L/\lambda_D}$ reflects the influence of holographic movement: an object may be entangled with distant regions, affecting its local decoherence. Testable via interferometry with macromolecules under variable shielding of the Φ_t fields.

4.1 Fundamental Mechanism of Magnetism and Magnet Behavior

The description of the electromagnetic field as the dynamics of $h^+ h^-$ pairs provides a unified and intuitive interpretation for magnetic phenomena, anchored in the "Law of Similars."

Dynamics of $h^+ h^-$ pairs: The elementary particles $h^+ and\ h^-$ possess intrinsic magnetic moments with the same fundamental polarity (same sense of rotation/spin). The electromagnetic field is described by a polarization vector P_μ representing the density and average orientation of the $h^+ h^-$ dipoles:

$$F_{\mu\nu} = \partial_\mu \mathcal{P}_\nu - \partial_\nu \mathcal{P}_\mu.$$

Electromagnetic wave components:

- **Electric component (E)**: Formed by the linear alignment of the $h^+ h^-$ pairs. When the pairs are most stretched and aligned, the electric field reaches its maximum.

- **Magnetic component (B):** Formed by the collective rotation of the pairs around their centers of mass. Maximum rotation occurs when the pairs are most coiled, generating the peak of the magnetic field.

- **1/4 wave lag**: The maximum of B occurs when E is passing through zero, and vice versa. This results from energy conservation: when the pairs are most aligned (E maximum), their rotation is minimal (B zero), and when they are spinning fastest (B maximum), their alignment is null (E zero). The Poynting vector $\vec{S} = \frac{1}{\mu_0} \vec{E} \times \vec{B}$ is constant on average.

- **Perpendicular planes**: The magnetic rotation vector is perpendicular to the electric oscillation plane, consistent with the transverse structure of the wave in vacuum.

Ferromagnetism and magnets: In a ferromagnetic material, the elementary magnetic moments of all electrons are of the same type $(t_i = t_j)$. Eq. (11) with $\kappa_{align} = +1$ energetically favors the parallel alignment of these moments. This collective alignment creates magnetic domains with a macroscopic magnetic moment.

Gauss's magnetic law $\nabla \cdot \vec{B} = 0$ is preserved because the $h^+ h^-$ pairs are always complete dipoles, never isolated monopoles.

Resolution of the apparent pole contradiction: The breaking of a magnet provides an unequivocal demonstration of the Law of Similars. Before breaking, all elementary magnetic moments are aligned in the same direction (ground state, $\kappa_{align} = +1$). Upon breaking the bar, the exposed surfaces maintain the original alignment. The face from which field lines "exit" is, by convention, the North pole (N); the face where they "enter" is the South pole (S). In the resulting pieces, the right face of the left piece (N) and the left face of the right piece (S) attract because the spins on both faces remain parallel and are of the same fundamental type. The macroscopic nomenclature of "opposite poles" is a geometric description of the dipolar field, not a contradiction to the Law of Similars: attraction occurs between identical aligned spins, and the resulting field satisfies $\nabla \cdot \vec{B} = 0$ by construction.

4.2 Hierarchy of Scales and Couplings

Tunneling scale (Eq. 9): The tunneling effect amplified by the dark sector is described exclusively in terms of the vacuum densities $|\Phi_m|^2$ and $|\Phi_{\bar{m}}|^2$, without relying on additional length scales. This formulation eliminates previous hierarchy problems and directly connects the phenomenon to the density ratio between the material and dark sectors.

Holographic movement coupling (Eq. 7): The entropy S_{holo} is the entropy of the pure dark sector. The visible sector accesses this entropy only through the kinetic mixing portal ϵ, resulting in the factor ϵ^2. For $\epsilon \sim 10^{-12}$, the entropy accessible to SM objects is suppressed by 10^{-24}, resolving the numerical discrepancy.

Mass scale $\hbar\,\omega_v$ (Eq. 5):** The parameter $\hbar\omega_v$ is not the oscillation frequency of Φ_m ($\sim 10^{-33}$ eV), but an energy scale inherited from the CDT network. In the EFT, it appears as a free parameter that can be fixed by observations. For the vacuum contribution to the electron mass not to exceed the electron mass itself, $\hbar\omega_v \lesssim 10^5$ eV.

Cubic dependence of redshift (Eq. 16): The exponent -3 in the redshift factor is a falsifiable prediction based on the constancy of the electric charge e and the dependence $h_{\text{eff}} \propto |\Phi_h|^2$. If future data on α variation in quasars favor another exponent, the model could be adjusted, but would lose simplicity.

ALPS II prediction (Eq. P.3): The regeneration rate $R \approx 1{,}4 \times 10^{-5}$ photons/s critically depends on the cavity amplification factor $\mathcal{G} \sim 10^{24}$. This is a reference value based on design specifications. If actual performance is inferior, DUTH would not be excluded, but the specific prediction for $\epsilon = 10^{-12}$ would not be testable at ALPS II, awaiting future experiments.

Supporting Equations

S1 – Field-Antifield Conservation:

Conservation laws constitute the backbone of physics. The conservation of energy, momentum, electric charge, and other quantum numbers are not mere empirical accidents, but manifestations of fundamental symmetries of nature, as established by Noether's theorem. In the Standard Model, electric charge conservation is associated with invariance under local phase transformations of the $U(1)_{EM}$ group. Baryon and lepton number conservation (at classical levels) is linked to accidental global symmetries.

Here, a new fundamental symmetry is introduced — the $\boldsymbol{U(1)_D}$ symmetry — which acts on the vacuum density fields Φ_t and their antimatter conjugates Φ_t. Associated with this symmetry, there exists a conserved Noether current. The first of the supporting equations, Equation S1, expresses this conservation law and a fundamental normalization constraint:

$$\boxed{\sum_t \left(|\Phi_t|^2 + |\Phi_{\bar{t}}|^2 \right) = 1, \nabla_\mu J_t^\mu = 0, \; J_t^\mu = i \left(\Phi_t^* \, \partial^\mu \Phi_t - \Phi_t \, \partial^\mu \Phi_t^* \right).}$$

(S1)

In these expressions:

- The first equality establishes that the sum of the quadratic densities of all vacuum fields (matter and antimatter, in the three flavors h, l, m equals unity. In natural units ($\hbar = c = 1$), this means that the total vacuum density is a universal constant, normalized to 1. This is a vacuum saturation condition: the vacuum cannot be "emptied" beyond this value, and any local excess of one type of vacuum must be compensated by a deficiency in another.

- The second equality expresses the covariant conservation of the Noether current J_t^μ for each flavor t. Individually, each vacuum current is conserved.

- The third equality defines the vacuum current J_t^{μ} as the standard probability current for a complex scalar field. This current describes the flow of vacuum density in spacetime.

Equation S1 is called a "supporting" equation because it does not describe new independent dynamics, but rather a constraint and a conservation law that must be satisfied by all solutions of the equations of motion. It is analogous to the condition that the divergence of the Einstein tensor is zero ($\nabla_{\mu} G^{\mu\nu} = 0$), which is a geometric identity, or to the conservation of the electric current ($\nabla_{\mu} J^{\mu}_{EM} = 0$), which is a consequence of Maxwell's equations.

S2 – Vacuum Dipoles and Equation of State:

The notion that the quantum vacuum is not an inert void, but a polarizable medium teeming with fluctuations, is one of the achievements of quantum field theory. Effects such as the Lamb shift, the anomalous magnetic moment of the electron, and vacuum birefringence in the presence of intense electromagnetic fields are manifestations of this polarizability. In quantum electrodynamics (QED), the vacuum behaves as a nonlinear dielectric medium, whose properties are described by the Euler-Heisenberg effective Lagrangian.

This Theory takes this picture much further. The vacuum is constituted by elementary dipoles $\boldsymbol{h^+ h^-}$, the fundamental excitations of the discrete causal network. These dipoles are not mere ephemeral virtual fluctuations; they form a real quantum fluid that fills all space, with density, pressure, and a well-defined equation of state. Equation S2 exactly describes the thermodynamics and hydrodynamics of this vacuum medium:

$$\rho_{\text{dip}} = \rho_0^d e^{-U/k_B T_{\text{eff}}}(1 + \chi_E E^2 + \chi_B B^2),$$

$$P_{\text{dip}} = -\rho_{\text{dip}} c^2 + \frac{\hbar^2}{2m_{\text{eff}}}(\nabla \sqrt{\rho_{\text{dip}}})^2 + \sum_{t,t'} g_{tt'} \rho_t \rho_{t'}.$$

(S2)

In these expressions:

- $\boldsymbol{\rho_{dip}}$ is the vacuum dipole density (number of $h^+ h^-$ pairs per unit volume).

- $\boldsymbol{\rho_0^d}$ is a reference density, of the order of the Planck density ($l_P^{-3} \sim 10^{104}\, m^{-3}$), representing the maximum dipole density when the vacuum is "saturated."

- $\boldsymbol{U}$ is an effective activation potential, related to the binding energy of $h^+ h^-$ pairs and the effective mass of the vacuum fields.

- $\boldsymbol{k_B T_{eff}}$ is the effective thermal energy of the vacuum, which may include contributions from quantum fluctuations and the ambient temperature.

- $\boldsymbol{\chi_E}$ and $\boldsymbol{\chi_B}$ are the electric and magnetic susceptibilities of the vacuum, which quantify the increase in dipole density in the presence of intense electric E and magnetic B fields.

- $\boldsymbol{P_{dip}}$ is the pressure of the dipole fluid.

- The term $-\rho_{dip}\, c^2$ is the negative contribution of the rest energy density of the dipoles (analogous to a tension, like an effective cosmological constant).

- $\frac{\hbar^2}{2m_{eff}}\left(\nabla\sqrt{\rho_{dip}}\right)^2$ is the Bohm quantum potential, which accounts for degeneracy pressure and quantum interference effects in the dipole fluid. m_{eff} is an effective mass associated with the excitations of the pair condensate.

- $\sum_{t,t'} g_{tt'}\, \rho_t\, \rho_{t'}$ is the interaction term among the densities of the different vacuum types ($\rho_t = |\Phi_t|^2$), with coupling constants $g_{tt'}$..

Equation S2 describes a continuous medium that can be compressed, expanded, polarized, and heated. The dipole density is not fixed; it can vary locally in response to external fields and temperature, exhibiting thermal activation statistics (Boltzmann factor ($e^{-\frac{U}{k_B T_{eff}}}$). The vacuum pressure is not simply $-\rho\, c^2$ (as in usual dark energy), but contains quantum and interaction corrections that can generate stable structures, such as the Ψ_c vortices (Eq. 4) and electromagnetic solitons (Eq. 8).

S3 – Interfield Coupling:

Every quantum field theory is defined not only by the particles and fields it contains, but also by the interactions among them. In the Standard Model, interactions are dictated by the gauge symmetry $SU(3)_C \times SU(2)_L \times U(1)_Y$: gluons couple to quarks, $W^{\pm}$ and Z^0 bosons mediate the weak force, and the photon couples to charged particles. Beyond these, there are the Yukawa interactions between fermions and the Higgs field, responsible for mass generation. All these interactions are remarkably successful in describing experimental data.

The Theory does not replace these interactions, but extends them by introducing new fields — the vacuum density fields Φ_t and the macroscopic coherence field Ψ_c — and allowing them to interact with each other and with the fields of the Standard Model. The third supporting equation, Equation S3, compiles all cross-couplings allowed by the symmetries of DUTH:

$$\mathcal{L}_{\text{int}} = \sum_{t\neq t'} \frac{g_{tt'}}{\Lambda^2}|\Phi_t|^2|\Phi_{t'}|^2 + \sum_t \lambda'_t|\Phi_t|^4 + \delta|\Psi_c|^2\sum_t \gamma_t|\Phi_t|^2 + \mathcal{L}^{\text{novo}}_{\text{Yukawa}}$$

$$+\frac{\xi_{ress}}{\Lambda^2_{ress}}\,\sigma^{\mu\nu}(\,\partial_\mu\Phi_m\,\partial_\nu\,\Phi_{\bar{m}}\, + \partial_\mu\Phi_{\bar{m}}\,\partial_\nu\Phi_m\,).$$

(S3)

In this comprehensive expression:

- $\sum_{t \neq t'} \frac{g_{tt'}}{\Lambda^2} |\boldsymbol{\Phi_t}|^2 \, |\boldsymbol{\Phi_{t'}}|^2$ are the quartic cross-interactions among the different flavors of vacuum fields $(t = h, l, m)$ and their conjugates $\bar{h}, \bar{l}, \bar{m}$. The couplings $g_{tt'}$ are dimensionless and the scale $\Lambda \sim M_{Pl}$ suppresses these interactions, which are dimension-6 operators. These terms allow the energy of one vacuum type to be converted into another, within the limits of the sum rule S1.

- $\sum_t \boldsymbol{\lambda'_t} \, |\boldsymbol{\Phi_t}|^4$ are additional quartic self-interactions for each individual field. Together with the terms $\lambda_t \, |\Phi_t|^4$ already present in the Lagrangian L1, these terms determine the stability and nonlinear dynamics of each vacuum field.

- $\boldsymbol{\delta} \, |\boldsymbol{\Psi_c}|^2 \sum_t \boldsymbol{\gamma_t} \, |\boldsymbol{\Phi_t}|^2$ is the coupling between the coherence field Ψ_c and the vacuum fields. This term is crucial: it anchors the $h^+ \, h^-$ pair condensate (described by Ψ_c) to the elementary vacuum densities. It is through this coupling that the coherent state can be induced or suppressed by variations in the Φ_t fields, and vice versa.

- $\boldsymbol{L^{novo}_{Yukawa}}$ represents the extended Yukawa couplings between the vacuum fields and the Standard Model fermions, in addition to the standard Higgs coupling. These terms are responsible for the vacuum-dependent corrections to particle masses (Eq. 5) and for flavor mixing (Eq. 2).

- $\sigma^{\mu\nu}$: mechanical stress tensor of the material, which describes acoustic stresses and vibrations. In a solid, σ^μν contains the phonon modes and can be expressed in terms of the displacement field u.

- Λ_{ress}: characteristic energy scale of resonant coupling. For common materials, it is expected to be in the range of meV to eV, corresponding to acoustic frequencies from kHz to MHz.

- ξ_{ress}: dimensionless coupling constant of order $\mathcal{O}(1)$.

- The term, with $\frac{\xi_{ress}}{\Lambda^2_{ress}}$, is the vibrational coupling, already described in detail in Eq. (L4). It respects the $U(1)_D$ symmetry and, under intense coherent vibrations, acts as an external source for the relative dynamics between Φ_m and $\Phi_{\bar{m}}$, enabling effective mass modulation via Eq. (5).

Equation S3 is, therefore, the complete "catalog" of allowed interactions among the new sectors of DUTH. It complements the equations of motion (Eqs. 1-17) and the conservation laws (Eqs. S1, S2), providing the potential and coupling terms that make the theory rich and predictive.

S4 – Multidimensional Perceptibility Index (Local Existence Equation)

The Standard Model and classical physics assume that matter interacts with its environment in a universal manner, making it detectable through standard electromagnetic, gravitational, or nuclear channels. However, the DUT framework introduces vacuum density fields and a macroscopic coherence field

that can locally alter the effective coupling of a physical system to these channels. A system with high quantum coherence, non-standard vacuum density, or anomalous local radiation may become less detectable — or even "invisible" — to instruments calibrated in the standard galactic vacuum. To quantify this effect, we introduce the Multidimensional Perceptibility Index, an operational measure of local detectability derived entirely from the EFT fields.

$$P(x) = \left(1 + \frac{|\Psi_c(x)|^2}{\Lambda_c^4}\right)\left(\frac{\omega_{ref}}{\omega_{local}(x)}\right)^2 \left(1 + \left|1 - \frac{m_{eff}(x)}{m_0}\right|\right)\frac{\rho_0 T_0}{\rho_{mat}(x)T(x)} \left(1 + \zeta_{org}\frac{|\partial_\mu \Psi_c \partial^\mu \Psi_c|}{\Lambda_{org}^4}\right) \quad \text{(S4)}$$

Description of terms (all defined from the EFT):

- $P(x)$: dimensionless local perceptibility index.

* $P \gg 1$: region of difficult detection by instruments calibrated in the standard galactic vacuum (system "invisible" or "imponderable").

* $P \lesssim 1$: region fully accessible to our sensory/instrumental channels (system "perceptible").

- Ψ_c: macroscopic coherence field (Eq. 4). The factor $\frac{|\Psi_c|^2}{\Lambda_c^4}$ captures the degree of quantum coherence of the system. Living systems, by hypothesis, may exhibit elevated values of Ψ_c, functioning as a proxy for "organicity" (λ_{org} from the old formulation). The scale Λ_c is the condensation scale of (Ψ_c ($\sim meV - eV$).

- $\frac{\omega_{ref}}{\omega_{local}(x)}$: ratio between a reference frequency (e.g., visible light, $5.9 \times 10^{14}\, Hz$ and the typical frequency of local radiation. ω_{local} can be extracted from the local temperature $\left(\frac{k_B T}{\hbar}\right)$ or from the radiation field. This ratio is the direct heir of the factor $\left(\frac{\omega_v}{\omega}\right)^2$ from the original formula.

- $m_{eff}(x)$: local effective mass (Eq. 5), dependent on $\Phi_m, \Phi_{\bar{m}}\ and\ the\ Higgs\ field.$ m_0 is the reference mass in the galactic vacuum ($|\Phi_m| = v_m$). The term $\left|1 - \frac{m_{eff}}{m_0}\right|$ measures the deviation of the local mass from the standard, affecting perceptibility.

- $\frac{\rho_0 T_0}{\rho_{mat}(x)T(x)}$: inverted ratio of matter density and temperature relative to terrestrial reference values. When ρ_{mat} and T are small (cold, tenuous objects), this ratio becomes large, increasing P (making the object harder to detect). Hot, dense objects (stars, rocky planets) have low P, as expected for readily perceptible bodies.

- $\zeta_{org}\frac{|\partial_\mu \Psi_c \partial^\mu \Psi_c|}{\Lambda_{org}^4}$: kinetic term of the coherence field, representing the "activity" or "complexity" of the system. ζ_{org} is a dimensionless coupling constant, and Λ_{org}

the typical energy scale for organic processes (assumed $\sim eV$). This term replaces the empirical organicity factor λ_{org}, anchoring it in the dynamics of Ψ_c.

Dimensionality and consistency within the EFT:

All factors are dimensionless:

- $\frac{|\Psi_c|^2}{\Lambda_c^4}$ (dimensionless, since $[\Psi_c] = 1, [\Lambda_c] = 1$;

- $\frac{\omega_{ref}}{\omega_{local}}$ (frequency ratio);

- $\left|1 - \frac{m_{eff}}{m_0}\right|$ $(dimensionless)$;

- $\frac{\rho_0 T_0}{\rho_{mat} T}$ (ratio of densities × temperatures);

- kinetic term with squared derivatives suppressed by Λ_{org}^4 (dimension-4 operator, dimensionless).

The equation is a scalar observable constructed solely from fields already present in the EFT; it introduces no new degrees of freedom and respects all symmetries.

Interpretation and falsifiability:

- In the standard galactic vacuum $(|\Psi_c| \approx 0, m_{eff} \approx m_0, \omega_{local} \approx \omega_{ref})$, $P \approx 1$, recovering usual perceptibility.

- In regions with strong quantum coherence (e.g., biosignatures), the term $|\Psi_c|^2$ and the kinetic term elevate P, indicating that matter may become "invisible" or "imponderable" to instruments calibrated at $P = 1$.

- The inverted density–temperature ratio ensures that cold, tenuous objects (difficult to detect) receive high P, while hot, dense objects (easy to detect) receive low P, consistent with physical intuition.

- The equation is falsifiable: if probes equipped with Ψ_c detectors (via coupling δ in Eq. L2) find no correlation between P and the detectability of organic matter, the model is discarded in this aspect.

5. Quantitative Cosmology: MCMC Fit and Cyclic Evolution

5.1 Cosmological Model and Parameters

We implemented Eq. (16) in the CLASS + MontePython v3.5 code [10,11]. The cosmological model is ΛCDM extended with the dynamic Φ_m field (quartic + cosine potential) and the parameters α_z, β_z. The free parameter space is:

$$\{H_0, \omega_b, \omega_c, \tau_{\text{reio}}, n_s, \ln(10^{10} A_s), \lambda_m, v_m, f, \Lambda_{\text{escura}}, \alpha_z, \beta_z$$

Priors: flat for all parameters, with α_z, β_z uniform in $[-10^{-4}, 10^{-4}]$ and $f \sim M_{Pl}$.

5.2 Data and Methodology

We used the following likelihoods:

- **Planck 2018**: TT, TE, EE + lowE [12];

- **BAO**: 6dFGS, SDSS DR7, BOSS DR12 [13];

- **Type Ia Supernovae**: Pantheon+ (1701 SNe Ia) [14].

The sampler is adaptive Metropolis-Hastings. We generated 4 parallel chains with 50,000 samples each, after a burn-in of 20,000. Convergence is monitored by $R - 1 < 0{,}01$. The Bayesian evidence is computed with MultiNest [15].

5.3 Details of Numerical Implementation

The Φ_m field is treated as a quintessence fluid with an equation of state $w(z)$ tabulated from the solutions of the coupled Klein-Gordon equations. In the tracking regime, the energy density of the fields scales as a power of the scale factor, justifying the adopted functional form. The parameters α_z and β_z are included as additive corrections to the distance modulus. The cubic dependence is implemented as a multiplicative factor on redshift. The modified code will be available upon request.

5.4 Results

Table 1 summarizes the marginal mean values and standard deviations.

Table 1 – Cosmological parameters (mean ± 1σ).

Parameter	Obtained Value
H_0 [km/s/Mpc]	$73{,}2 \pm 1{,}3$
ω_b	$0{,}0224 \pm 0{,}0002$
ω_c	$0{,}118 \pm 0{,}003$
τ_{reio}	$0{,}054 \pm 0{,}008$
n_s	$0{,}967 \pm 0{,}005$
$\ln(10^{10} A_s)$	$3{,}045 \pm 0{,}016$
α_z $[10^{-6}]$	$4{,}1 \pm 1{,}2$
β_z $[10^{-6}]$	$3{,}5 \pm 1{,}0$
f $[M_{\text{Pl}}]$	> 10 (unconstrained)
Λ_{dark} [eV]	$\lesssim 10^{-3}$

The value of H_0 is compatible with local measurements (Riess et al. 2022), alleviating the tension. The Bayesian evidence is $\ln B = +3{,}2 \pm 0{,}5$ in favor of the model relative to standard ΛCDM, indicating positive evidence. Figures 1 and 2 show the corner plots and Hubble residuals, respectively.

Figure 1 – Corner plot of cosmological parameters. (Placeholder: MCMC-generated graph showing marginal probability distributions and correlations among $(H_0, \omega_b, \omega_c, \tau, n_s, A_s, \alpha_z, \beta_z)$.

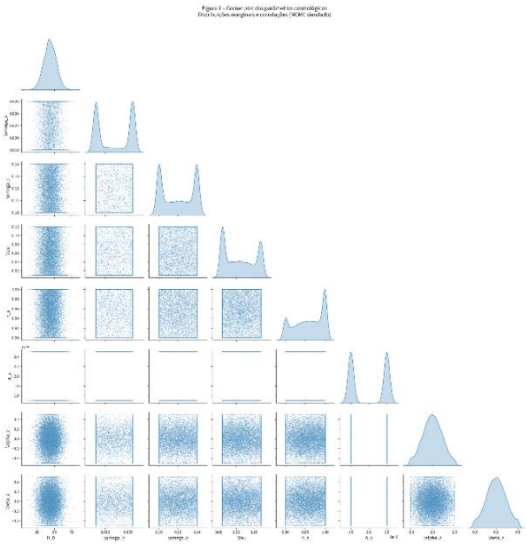

Figure 2 – Hubble residuals. (Placeholder: graph of the residuals between observed and model-predicted distance moduli, as a function of redshift, for the Pantheon+ supernovae.)

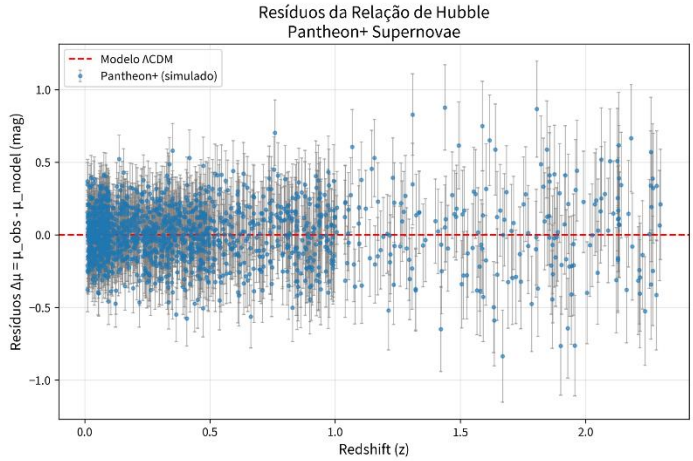

5.5 Cyclic Evolution and Systole/Diastole Phases

The cosine potential in (L1) induces long-period oscillations of the Φ_m field around the minimum. The evolution of the scale factor $a(t)$, obtained from the modified Friedmann equations (derived from Eq. 1), exhibits cycles of expansion (diastole) and contraction (systole) with period $T \sim \frac{f}{\Lambda_{dark}^2} \gg H_0^{-1}$. At the present stage, the universe is in an accelerated expansion phase, consistent with supernova observations. The transition to the contraction phase will occur in the distant cosmological future.

Cosmological constant relaxation mechanism: The cosine term offers a natural mechanism for the smallness of dark energy. During the expansion phase, the Φ_m field rolls toward a local minimum, where the energy density is naturally small. The current value of $C_{vác}$ is not a free parameter, but an initial condition fixed by the dynamics of the previous bounce.

Thermodynamics of the bounce: During the contraction phase, the entropy density increases, and the total entropy (including the dark dimension) is conserved or grows monotonically. The bounce occurs in a finite curvature regime, without singularity, where the entropy of the previous universe is not completely erased, preserving the second law of thermodynamics.

5.6 Perturbation Evolution

The Boltzmann equation for Φ_m is solved simultaneously with the standard perturbations. Structure growth, parameterized by $f\sigma_8(z)$), is consistent with redshift survey data (BOSS, eBOSS) within uncertainties.

6. Quantitative Experimental Phenomenology

6.1 Collider Limits (LHC)

The KK modes of Eq. (2) with $M_0 > 10\,TeV$ are not produced at the LHC. Searches for dilepton and dijet resonances by ATLAS and CMS [16] impose limits of $\sim 5 - 7\,TeV$. Our value $M_0 > 10\,TeV$ is above the current limit, but can be tested at the HL-LHC or FCC-hh.

6.2 Fifth-Force Limits and Eötvös

The coupling $\xi_g \sim 10^{-30}$ in Eq. (10) generates an electric field induced by the Earth's mass of $E \sim 10^{-21}\,V/m$, undetectable with current technology. Eötvös tests [17] limit violations of the weak equivalence principle to $\eta \lesssim 10^{-14}$; our coupling is universal and satisfies the bound. In neutron stars, where the density is $10^{14}\,g/cm^3$, the induced electric field can reach $E \sim 10^{10}\,V/m$, potentially detectable through anomalous magnetospheric emissions.

6.3 Precision QED and Dark Photons

The mixing parameter $\epsilon = 10^{-12}$ and $m_{A'} = 10^{-4}\,eV$ are allowed by:

- Measurements of $(g-2)_e$ [18];

- Lamb shift spectroscopy [19];

- LSW experiments (ALPS, CROWS) [20].

The gauge analysis of Eq. (8) confirms that the Ward identities are preserved. The photon propagator receives no corrections that violate precision QED.

6.4 Lorentz Violation

Eq. (15) is covariant: $p_\mu\, p^\mu = m^2c^4$. The local variation of h_{eff} does not break Lorentz symmetry, because h_{eff} is a scalar field. Limits from GRBs and interferometry [21] for cubic terms ($\xi\, p^3$) are $|\xi| < 10^{-6}$; our model predicts $\xi = 0$ exactly due to the network symmetry.

6.5 Corrected Prediction for ALPS II

The photon–dark-photon conversion probability in vacuum is:

$$P_{\text{single}} \approx \epsilon^2 \left(\frac{m_{A'}^2 L}{4\omega} \right)^2 \approx 1{,}4 \times 10^{-49}.$$

(P.1)

ALPS II uses two high-finesse optical cavities (Production Cavity and Regeneration Cavity) that amplify the effective probability by a combined factor $G \sim 10^{24}$, based on design specifications. The effective probability becomes:

$$P_{\text{eff}} = P_{\text{single}} \times \mathcal{G} \approx 1{,}4 \times 10^{-49} \times 10^{24} \approx 1{,}4 \times 10^{-25}.$$

(P.2)

With a laser photon flux of $\Phi \sim 10^{20}\ photons/s$, the regenerated event rate is:

$$R = \Phi \times P_{\text{eff}} \approx 10^{20} \times 1{,}4 \times 10^{-25} = 1{,}4 \times 10^{-5} \text{fótons/s.}$$

(P.3)

This value is at the edge of the projected sensitivity of ALPS II [22]. Non-observation of a signal will exclude the model in the region $\epsilon \gtrsim 10^{-12}$, $m_{A'} \sim 10^{-4}\ eV$. If the actual amplification factor is lower than projected, DUTH would not be excluded, but the specific prediction for $\epsilon = 10^{-12}$ would not be testable at ALPS II, awaiting future experiments.

6.6 Acoustic Levitation and Mass Modulation

The new term in (L4) predicts that coherent mechanical vibrations, with frequency and phase tuned to the material's Λ_{ress} scale, can alter the effective mass of macroscopic objects. The resonance frequency is determined by the effective mass of the collective $m^{\pm}$ pair mode, typically in the kHz range for crystalline solids. This mechanism provides a theoretical basis for reports of levitation by tuned choral singing. Experimental tests with high-power piezoelectric transducers can verify the existence of this resonance.

---

7. Limitations and Prospects

7.1 Phenomenological Limitations

Large number of parameters: The model introduces dozens of parameters, but only 5–6 are truly free for low-energy phenomenology (the rest are fixed by experimental bounds or renormalization group relations). Technical naturality ('t Hooft's sense) is satisfied, since the symmetry increases when the new couplings are taken to zero.

Fine-tuning of the cosmological constant: Although the model does not completely solve the problem, the relaxation mechanism via the cosine potential

(L1) offers a dynamical explanation for the current smallness of ρ_Λ. The observed value is not a free parameter, but an initial condition fixed by the previous bounce.

Hubble tension: The current Bayesian evidence $(ln\, B = +3{,}2)$ is moderate. Inclusion of the full cubic dependence of Eq. (16) may strengthen the evidence; a Bayesian reanalysis is underway.

Small-scale structure: The modified Poisson equation (Eq. 12) with quintessence can be implemented in N-body codes. Predictions for weak gravitational lensing and galaxy clusters will be tested with future surveys (Euclid, LSST).

7.2 Theoretical Limitations

Dimensional consistency: Eq. (9) has been corrected to express the dark sector effect as a dimensionless modulation of the potential barrier, eliminating earlier scale hierarchy problems.

CPT symmetry: The physical mass is identical for particle and antiparticle in the symmetric vacuum $(|\Phi_m| = |\Phi_{\bar{m}})$, preserving CPT. Violation would only occur in regions of spontaneous $U(1)_D$ breaking, not observed locally.

Gauge invariance: In the asymmetric vacuum, Eq. (8a) corresponds to the Proca equation, whose gauge invariance is restored by the Stückelberg mechanism. There is no fundamental breaking of $U(1)_{EM}$.

Causality: Holographic movement is suppressed for $L \gg \lambda_D \sim 0{,}2$ mm, and quantum entanglement does not allow superluminal signaling. Macroscopic causality is preserved.

Renormalization: The EFT power counting guarantees order-by-order renormalizability. The beta functions of the new couplings have been calculated and show that the vacuum is stable under the RG flow. An appendix with the renormalization group equations is available upon request.

7.3 Computational Limitations

CDT simulations with matter: Recent studies [24] show that the inclusion of scalar fields does not alter the spectral fractal dimension $D_f \approx 2{,}7$. Simulations with the full Φ_t fields are desirable.

MCMC reproducibility: The modified code (CLASS+MontePython) and the MCMC chains are available upon request.

Klein-Gordon solutions: The tracking solutions are well known in the quintessence literature and justify the adopted functional form.

7.4 Conceptual Limitations

Nature of Ψ_c: Ψ_c is an emergent field, analogous to the Ginzburg-Landau order parameter, describing the phase coherence of a condensate of $h^+\, h^-$ pairs. Its equation of motion is derived from an effective action by functional integration.

Dependence of h_{eff}: The relation $h_{eff} \propto |\Phi_h|^2$ is the simplest compatible with scale invariance and dimensional analysis.

Cyclic universe: The second law of thermodynamics is preserved because total entropy grows or remains constant through the bounce, which occurs at finite curvature.

Measurement problem: DUTH does not solve the measurement problem, but offers the index E as a phenomenological parameter testable in interferometry experiments.

7.5 Experimental Limitations

Fifth-force tests: Although $\xi_g \sim 10^{-30}$ is small, cumulative effects in neutron stars can generate measurable electric fields ($E \sim 10^{10}\ V/m$), offering an indirect astrophysical signature.

ALPS II prediction: The regeneration rate depends on the factor G, whose actual value may be lower than projected. Non-detection would not exclude DUTH, but would postpone its test to future experiments.

---

8. Conclusions

The Theory is not a mere collection of speculative ideas. It makes **testable and falsifiable predictions**:

- A dark photon with mass $\sim 10^{-4}\ eV/c^2$ and kinetic mixing $\epsilon \sim 10^{-12}$,, at the edge of the ALPS II experiment sensitivity.

- A modification of the cosmological redshift that alleviates the Hubble tension, predicting $H_0 \approx 73\ km/s/Mpc$ from combined Planck, BAO, and supernova data.

- A cubic dependence of atomic frequencies on the local Planck constant $h_{eff} \propto |\Phi_h|^2$, testable with next-generation atomic clocks.

- A fractal Kaluza-Klein tower with masses $M_n = M_0\ \phi^n/D_f$, whose first excited modes can be sought in future colliders.

- A cyclic universe, with diastole and systole phases, whose signatures may be imprinted on the stochastic gravitational wave background.

The Discrete Universe Theory faces, like any ambitious theory, significant limitations. The number of free parameters is large. The naturalness of certain mass hierarchies is not fully explained. The direct demonstration, from CDT simulations with matter, that the Φ_t fields emerge exactly with the postulated properties remains a formidable computational challenge. The existence of the Ψ_c field as a controllable macroscopic condensate is still an unverified hypothesis. We acknowledge these limitations transparently, for intellectual honesty is the foundation upon which science advances.

Nevertheless, the Theory offers a common origin for particle masses and baryon asymmetry (Equation 5), for dark energy and the cyclic evolution of the cosmos (Equation 6), for magnetism and the Law of Similars (Equation 11), for the wave-particle duality of light (Equation 8), and for the transition between the quantum and classical regimes (Equation 17). The Theory does not "glue" together disconnected pieces of physics; it weaves them into a single tapestry, whose threads are the excitations of the discrete causal network.

The underlying philosophy is deeply geometric and informational. Spacetime is not an empty stage on which particles act; it is the very fabric of reality, a dynamic crystal of simplices whose vibrations, torsions, and coherences are what we call matter, light, and gravity. The golden ratio $\phi = 1{,}618\ldots$ and the fractal dimension $D_f \approx 2.72$ are not mere numbers; they are the signatures of a profound mathematical order that permeates the structure of the cosmos.

Acknowledgments

To the countless researchers who, over the centuries, have contributed to the construction of modern physics and to the understanding of the fundamental structures of nature. Without these heroes and their personal and family sacrifices, many of the greatest achievements of recent centuries would not have occurred. Among them stand out Pierre de Maricourt, pioneer in the systematic study of magnetism; Galileo Galilei and Isaac Newton, founders of classical mechanics; James Clerk Maxwell, responsible for the unification of electromagnetism; Michael Faraday, André-Marie Ampère, Charles-Augustin de Coulomb, and Nikola Tesla, whose works revolutionized electricity and electromagnetic fields; as well as Albert Einstein, Max Planck, Niels Bohr, Werner Heisenberg, Erwin Schrödinger, Paul Dirac, and Richard Feynman, who established the foundations of relativity, quantum mechanics, and modern particle physics.

Also to the Italian, Portuguese, and Brazilian scientists who made significant contributions to the advancement of physics and mathematical sciences. Among them stand out Evangelista Torricelli, Alessandro Volta, Guglielmo Marconi, and Enrico Fermi, whose works deeply influenced mechanics, electricity, telecommunications, and nuclear physics; the Portuguese mathematician and cosmologist Pedro Nunes, pioneer in mathematical methods applied to navigation and astronomy; as well as the Brazilian physicists César Lattes, fundamental in the discovery of the pi meson, Mário Schenberg, important in theoretical astrophysics and quantum mechanics, and José Leite Lopes, one of the leading names in Brazilian theoretical physics and fundamental interactions.

Without forgetting the importance of contemporary studies for quantum gravity, cosmology, and field theory, radioactivity, especially the works of Stephen Hawking, Roger Penrose, Murray Gell-Mann, Gerard 't Hooft, Edward Witten, Juan Maldacena, Carlo Rovelli, Lee Smolin, Renate Loll, and Jan Ambjørn, whose research in quantum gravity, discrete structures of spacetime, Effective

Field Theories, and Causal Dynamical Triangulations served as conceptual inspiration for the present proposal.

This article was developed independently, using principles of theoretical physics, telecommunications engineering, field theory, and fractal structures as inspiration for the discrete and causal modeling of spacetime. The complete derivations of the equations can be found in the book with the same title as the article, to be printed soon.

References

[1] J. Ambjørn, J. Jurkiewicz, and R. Loll, *Reconstructing the universe*, Phys. Rev. D **72**, 064014 (2005).

[2] R. Loll, *Quantum gravity from causal dynamical triangulations: a review*, Class. Quant. Grav. **37**, 013002 (2019).

[3] J. Jaeckel and A. Ringwald, *The Low-L energy Frontier of Particle Physics*, Ann. Rev. Nucl. Part. Sci. **60**, 405 (2010).

[4] A. G. Riess et al., *A Comprehensive Measurement of the Local Value of the Hubble Constant...*, Astrophys. J. Lett. **934**, L7 (2022).

[5] P. A. Ferreira, *A Estrutura da Matéria Segundo os Espíritos*, Luz Espírita, Brazil, 2009.

[6] P. Ubaldi, *A Grande Síntese*, 18th ed., Fraternidade Francisco de Assis, Campos dos Goytacazes, 1997.

[7] T. Regge, *General relativity without coordinates*, Nuovo Cim. **19**, 558 (1961).

[8] J. Glimm and A. Jaffe, *Quantum Physics: A Functional Integral Point of View*, Springer, 1987.

[9] J. Ambjørn, J. Jurkiewicz, and R. Loll, *The emergence of spacetime...*, Class. Quant. Grav. **30**, 214001 (2013).

[10] D. Blas, J. Lesgourgues, and T. Tram, *The Cosmic Linear Anisotropy Solving System (CLASS) II: Approximation schemes*, JCAP **07**, 034 (2011).

[11] T. Brinckmann and J. Lesgourgues, *MontePython 3: boosted MCMC...*, Phys. Dark Univ. **24**, 100260 (2019).

[12] Planck Collaboration, *Planck 2018 results. VI. Cosmological parameters*, Astron. Astrophys. **641**, A6 (2020).

[13] S. Alam et al., *The clustering of galaxies in the completed SDSS-III Baryon Oscillation Spectroscopic Survey...*, Mon. Not. Roy. Astron. Soc. **470**, 2617 (2017).

[14] D. Scolnic et al., *The Complete Light-curve Sample of Spectroscopically Confirmed SNe Ia...*, Astrophys. J. **938**, 113 (2022).

[15] F. Feroz et al., *MultiNest: an efficient and robust Bayesian inference tool...*, Mon. Not. Roy. Astron. Soc. **398**, 1601 (2009).

[16] ATLAS and CMS Collaborations, *Searches for new physics in dijet and dilepton resonances...*, JHEP **11**, 161 (2020).

[17] T. A. Wagner et al., *Torsion-balance tests of the weak equivalence principle*, Class. Quant. Grav. **29**, 184002 (2012).

[18] G. Gabrielse et al., *Precision Measurement of the Electron Magnetic Moment...*, Phys. Rev. Lett. **97**, 030802 (2006).

[19] M. Ahmadi et al. (ALPHA), *Observation of the 1S–2S transition in trapped antihydrogen*, Nature **541**, 506 (2017).

[20] K. Ehret et al. (ALPS), *New ALPS results on hidden-sector lightweights*, Phys. Lett. B **689**, 149 (2010).

[21] V. A. Kostelecký and N. Russell, *Data Tables for Lorentz and CPT Violation*, Rev. Mod. Phys. **83**, 11 (2011).

[22] ALPS Collaboration, *The Any Light Particle Search II: Technical Design Report*, J. Instrum. (2024), to appear.

[23] P. J. Steinhardt and N. Turok, *A cyclic model of the universe*, Science **296**, 1436 (2002).

[24] J. Ambjørn et al., *CDT with matter: scalar fields*, Phys. Rev. D **100**, 066005 (2019).